

## Amorphous Metallic Alloys for Oxygen Reduction Reaction in a Polymer Electrolyte Membrane Fuel Cell

R. Gonzalez-Huerta<sup>1,\*</sup>, I. Guerra-Martinez<sup>1</sup>, J. Santiago Lopez<sup>1</sup>, A.R. Pierna<sup>2</sup> and O. Solorza-Feria<sup>3</sup>

<sup>1</sup>Instituto Politécnico Nacional, ESIQIE, Laboratorio de Electroquímica, UPALM, Ed.7, 07830, México D.F. Mexico

<sup>2</sup>Chemical Engineering and Environment Department. University of the Basque Country, Plaza de Europa, 20018 San Sebastián. Spain

<sup>3</sup>Depto. Química, Centro de Investigación y de Estudios Avanzados del IPN, A. Postal 14-740, 07360 México, D.F. Mexico

Received: November 20, 2009, Accepted: February 27, 2010

**Abstract:** Amorphous alloyed compounds have been used as electrode materials in electrochemical energy conversion devices. An interesting and important goal for their applications in polymer electrolyte membrane fuel cells is the optimization of the electrocatalysts loading in the membrane electrode assemblies (MEAs). Kinetics of the oxygen reduction reaction (ORR) on  $Ni_{59}Nb_{40}Pt_{0.6}Ru_{0.4}$ ,  $Ni_{59}Nb_{40}Pt_{0.6}Sn_{0.4}$  and  $Ni_{59}Nb_{40}Pt_{0.6}Ru_{0.2}Sn_{0.2}$  amorphous catalysts synthesized by mechanical milling were investigated in 0.5M  $H_2SO_4$  at 25°C. The electrocatalytic activity of ink thin-film type electrodes evaluated by cyclic voltammetry (CV) and rotating disk electrode (RDE) showed that the  $Ni_{59}Nb_{40}Pt_{0.6}Sn_{0.4}$  amorphous electrocatalyst was the most active from the three electrodes for the cathodic reaction. Fuel cell experiments were conducted at various temperatures at 30 psi for  $H_2$  and at 34 psi for  $O_2$ . MEAs fabricated using Nafion<sup>®</sup> 115 membrane and amorphous  $Ni_{59}Nb_{40}Pt_{0.6}Sn_{0.4}$  dispersed on carbon powder was tested as cathode electrocatalyst ( $1\text{ mg cm}^{-2}$ ) in a single polymer electrolyte membrane fuel cell, generating a power density of  $156\text{ mW cm}^{-2}$  at 0.43V and 80°C.

**Keywords:** Amorphous alloy, Electrocatalyst, Oxygen reduction, Fuel Cell.

### 1. INTRODUCTION

Mechanical alloying is an interesting high energy process for the preparation of a lot materials and specially amorphous alloys, which can be applied as electrodes in electrochemical energy conversion. Fuel cells, mainly direct methanol fuel cells (DMFCs) and polymer electrolyte membrane fuel cells (PEMFCs), are up to now one of the most attractive areas of research because they represent an important environmentally clean and friendly energy source [1-5]. Worldwide interest in clean energy generation systems has motivated research on the synthesis, characterization and evaluation of novel and stable oxygen reduction electrocatalysts for the direct four-electron transfer process to water formation [6-8]. In electrocatalysis, the oxygen reduction reaction, ORR, is a kinetically slow electrochemical reaction and it leads to higher reduction overpotential, due to the fact that the oxygen-oxygen bond (O-O) in the dioxygen molecule requires higher bond dissociation energy than other molecules. One of the targets on the cathode electrode is to reduce the platinum content in the PEM fuel cell, increasing or

maintaining the electrocatalytic performance with stability for a long time. Bimetallic and alloy catalysts have been a particularly active area of research because of the established fact that for the cathode reaction, multi-metallic surfaces have superior activity compared to pure platinum. The aim of this work is to investigate the kinetics of the oxygen reduction reaction (ORR) in 0.5M  $H_2SO_4$  on  $Ni_{59}Nb_{40}Pt_{0.6}Ru_{0.4}$  (PtRu),  $Ni_{59}Nb_{40}Pt_{0.6}Sn_{0.4}$  (PtSn) and  $Ni_{59}Nb_{40}Pt_{0.6}Ru_{0.2}Sn_{0.2}$  (PtRuSn) amorphous catalysts synthesized by mechanical milling following a procedure previously reported [3,9-11]. The use of amorphous materials arises primarily because of its corrosion resistance due to there is no grain boundary between the metallic elements. Studies have been reported showing that alloy materials present catalytic activity towards ORR, where amorphous catalysts were tested as carbon paste electrodes [9,10]. In this work ink-type thin-film electrodes were used and the electrochemical studies were performed by cyclic voltammetry (CV) and rotating disk electrode (RDE). After the electrochemical analysis were carried out, the study of the prepared amorphous alloys as cathodes electrocatalysts was performed in a membrane-electrode assembly (MEA) of a single polymer electrolyte fuel cell, as a complimentary part of this work.

\*To whom correspondence should be addressed:

Email: rosgonzalez\_h@yahoo.com.mx Phone: 57296000, ext. 55392

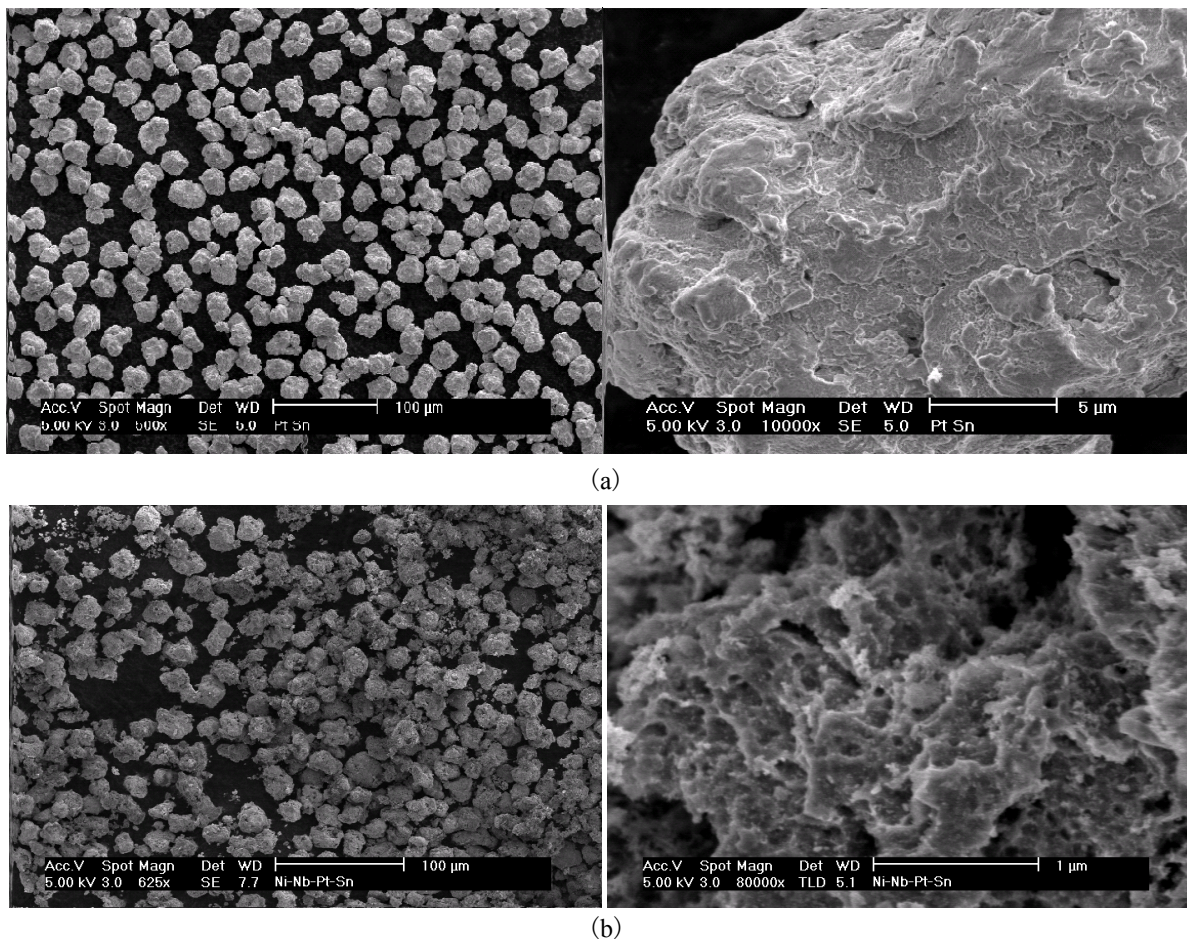


Figure 1. SEM images of PtSn amorphous metallic alloys: a) as synthesized and b) after a chemical activation in a HF 48 vol% solution.

## 2. EXPERIMENTAL

### 2.1. Catalyst synthesis and physical characterization

The preparation of the catalytic powder was performed by mechanical milling technique for a time of 40 h, as described in literature [3,11]. In all the cases, after the preparation, the catalytic powders were chemical activated introducing them in a 48 % v/v HF solution for 25 s at room temperature for eliminating superficial oxides. Afterwards, the powders were settled and rinsed with water three times to eliminate HF, dried and placed in a closed plastic recipient prior to their utilization. Scanning electron microscopy (SEM) was used to determine powder size and morphology before and after the chemical activation in HF. This was done in a Sirion FEG-SEM (from FEI) [11].

### 2.2. Electrode preparation for RDE study and electrochemical set-up

The electrochemical measurements were performed by using the conventional single compartment of a three-electrode array. A platinum mesh was used as the counter electrode and Hg/Hg<sub>2</sub>SO<sub>4</sub>/0.5M H<sub>2</sub>SO<sub>4</sub> (MSE=0.680V/NHE) as the reference electrode. A potentiostat/galvanostat (EG&G Mod. 263A) and a

Pine MSR rotation speed controller were used connected to a PC for control and data acquisition. A 0.5 M H<sub>2</sub>SO<sub>4</sub> electrolyte (pH=0.3) was prepared from distilled water. Cyclic voltammetry (CV) and rotating disk electrode (RDE) measurements were conducted on a thin film catalysts deposited on a RDE0008 glassy carbon disk electrode with a cross-sectional area of 0.19 cm<sup>2</sup>. The glassy carbon working electrode disk was prepared according to a method previously reported [2,4,12]. A thin film was deposited from a solution prepared by adding 8 ml of a resulting suspension from a mixture of 50 ml of an alcoholic solution containing 8 μl of Nafion® (5 wt.%, Du Pont, 1000 EW), 1 mg of chemical activated amorphous metallic alloys and 0.2 mg of Vulcan carbon XC-72. The resulting mixture was sonicated for 20 min and the resulting catalytic ink was deposited onto the glassy carbon surface. The estimated amount of catalyst on the electrode surface was about 0.72 mg cm<sup>-2</sup>. The working electrode was activated in an oxygen free electrolyte, by scanning the potential in a region between 1.7V/NHE to 0.0V/NHE at 100 mV s<sup>-1</sup> and 40 cycles. Thereafter, the acid electrolyte was saturated with pure oxygen and maintained on the electrolyte surface during the electrochemical experiments. Hydrodynamic experiments were performed at a speed rotation in the range of 100-1600 rpm at 5 mV s<sup>-1</sup>. All potentials are referred to NHE.

### 2.3. Preparation and characterization of the membrane-electrode assembly

A three layers structure (diffusion, catalyst and monomer) was used to prepare the membrane electrode assembly (MEA). Nafion<sup>®</sup> 115 (Dupont Fluoro Products) was used as a polymer electrolyte membrane, which was treated by a consecutive boiling processes for 1 h in 3% H<sub>2</sub>O<sub>2</sub>, 2M H<sub>2</sub>SO<sub>4</sub> and deionized water, according to the procedure previously described [7]. Before spraying, membranes were dried and flattened. Cathodic catalytic inks were prepared by mixing and sonicating a suspension formed by the electrocatalysts alloys, Vulcan carbon, Nafion solution and ethanol. The commercial electrode (1 mg 10 wt% Pt/C, E-TEK Electrochem) was used in the anode side of the assembly. Each MEA was prepared by spraying the corresponding catalyst ink on the cathodic side of the pretreated Nafion 115 membrane. The catalyst load at the cathode side was about 0.2 mg<sub>Pt</sub> cm<sup>-2</sup>. The MEA was prepared by placing the gas diffusion layer (carbon cloth) above the electrode at the cathodic side and the commercial electrode at the anodic side of the Nafion 115 membrane, followed by a hot-pressing of the assembly at 120 °C and 11 kg cm<sup>-2</sup> for 1.5 min. The effective electrode area for the anode and cathode sides was 5 cm<sup>2</sup>. The MEAs were tested with a commercial fuel cell system (CompuCell GT, Electrochem 890B) in a single cell rig with 5 cm<sup>2</sup> active geometrical area. The gas pressures (gp) at the anode and cathode sides were kept at 30 psi for H<sub>2</sub> and 34 psi for O<sub>2</sub>, respectively. The fuel cell test station was operated with high purity H<sub>2</sub> and O<sub>2</sub> at 100 cm<sup>3</sup> min<sup>-1</sup>. The temperature of the humidified reactant gases was kept 5 °C above the temperature of the cell. The performance was measured under steady-state conditions from 25 to 80 °C.

## 3. RESULTS AND DISCUSSION

### 3.1. Catalyst characterization

Before and after the chemical activation the morphology of the powders is different, as it is observed in figure 1. The morphology of the powder of PtSn before a chemical activation in a HF 48% solution by the SEM technique is displayed in figure 1(a). At this low magnification the powders appear clearly separated and compact irregular particles of different sizes, ranging from 20 to 30 μm the largest to about 5 μm the smallest ones. It is necessary to enhance that the aforementioned morphology is similar for PtRu and PtRuSn samples and also that only for PtRu can be observed the largest particle sizes, reaching 50 μm. The figure 1(b) shows the powder of PtSn after the chemical activation, which shows a porous surface and no significant difference in particle size. The difference is explained by the fact that during the chemical activation the superficial oxides are eliminated. The chemical activation is important because it generates active sites on the electrode surface. Electrochemical measurements were performed using the synthesized powders before activation and they did not present electrochemical activity.

### 3.2. Electrochemical characterization

Figure 2 presents a final voltamperometric cyclic activation for the PtSn, PtRu and PtRuSn amorphous electrocatalysts thin film electrodes, in the 0.5 M H<sub>2</sub>SO<sub>4</sub> nitrogen purged solution at 100 mVs<sup>-1</sup> scan rate. In this experiment the electrodes were submitted to 40 cycles in order to obtain reproducible voltammograms. The current density was normalized to surface geometric area. The

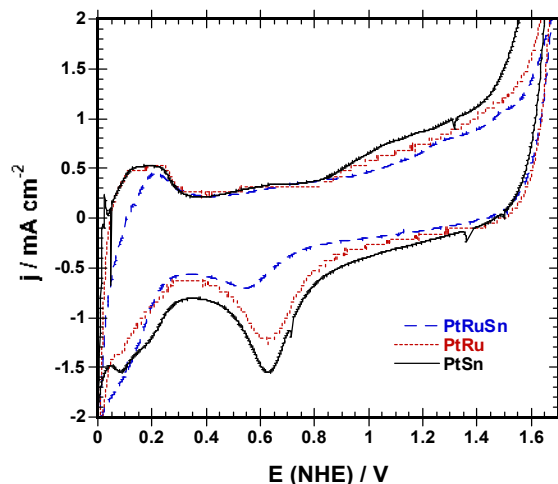


Figure 2. Cyclic voltammetry of PtSn, PtRu and PtRuSn amorphous catalysts in oxygen free 0.5 M H<sub>2</sub>SO<sub>4</sub> at 25°C. Scan rate potential of 100 mV s<sup>-1</sup>.

curves for the three catalysts show typical characteristics of Pt particles, where the hydrogen region is clearly attenuated but even visible. The proton adsorption/desorption section is depicted in 0.35-0.0 V/NHE potential range. Analysis at a more positive potential, corresponding to the anodic region also shows a well-defined hydroxide-desorbed reduction peak with the same electrochemical behavior as that observed for amorphous Pt catalyst dispersed in carbon paste electrodes [9,10]. The PtSn amorphous catalyst shows a better capability for anion adsorption compared to PtRu and PtRuSn catalysts, which also show lower current density attributed to the reduced distribution of the active sites on the electrode surfaces.

The RDE measurements of PtSn catalyst for the ORR in the oxygen saturated 0.5M H<sub>2</sub>SO<sub>4</sub> solution at 25°C, in the range of 0.90-0.20 V/NHE are shown in figure 3(a). One of the main characteristics in the polarization curves for Pt based particles incorporated into a Nafion<sup>®</sup> membrane is the well defined three processes: charge transfer control, mixed and mass transfer region. Results of steady-state current density-potential curves of figure 3(a) show a charge-transfer kinetics control region in the range of 0.90-0.75 V/NHE, a mixed control in the range of 0.75V-0.55V/NHE and at more cathodic potentials, mass transport became significant because of a well-defined transport-limited current dependence as a function of the speed rotation. PtRu and PtRuSn compounds reflect similar results for polarization curves (not depicted here) with the next slight differences: first, the current plateau is more inclined and second, the current density is lower than PtSn. It is considered that the decrease in the limiting current is associated with the decrease of oxygen diffusion through the electrode surface and when the distribution of active sites is less uniform and the electrocatalytic reaction is slower, the current plateau is more inclined. According to these behaviors, analysis of the hydrodynamic results has been made.

From the data of figure 3(a), the Koutecky-Levich plots ( $j^{-1}$  versus  $\omega^{-1/2}$ ) were drawn, figure 3(b). At all the rotation speeds, a se-

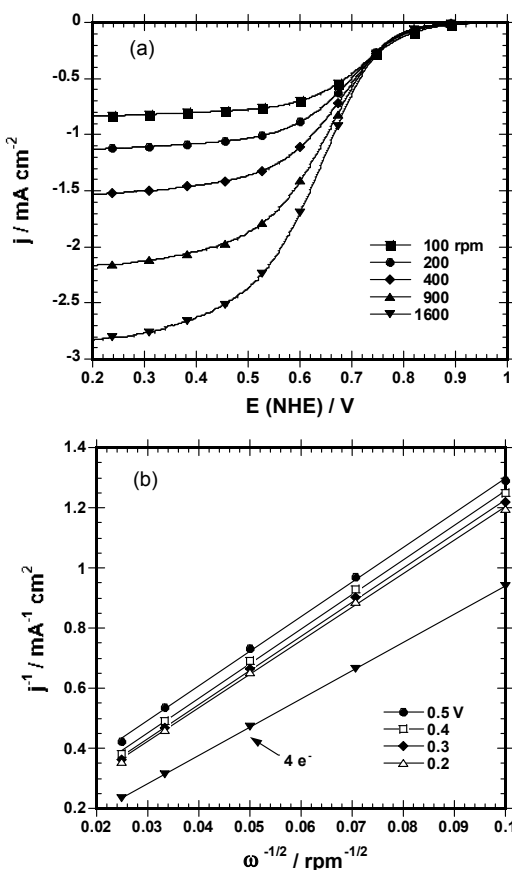


Figure 3. a) Current-potential curves for the molecular ORR on a PtSn electrocatalyst thin film electrode in oxygen saturated 0.5M H<sub>2</sub>SO<sub>4</sub> and b) Koutecky-Levich plots represented experimental and theoretical behaviors.

ries of essentially parallel straight lines in a broad potential range is illustrated in this figure, which indicates a first-order reaction for the O<sub>2</sub> reduction on the PtSn alloy electrode. Parallelism of the straight lines in figure 3(b) also indicates that the number of electrons transferred per O<sub>2</sub> molecule and active surface area for the reaction not change significantly within the potential range studied. The experimental average slope value of those lines in figure 3(b) is  $9.0 \times 10^{-2} \text{ mA cm}^{-2} \text{ rpm}^{-1/2}$ , considering that the current density is related to the geometric area of the electrode surface. The theoretical slope calculated with the parameters described above for the transfer of four electrons is  $9.41 \times 10^{-2} \text{ mA cm}^{-2} \text{ rpm}^{-1/2}$ . The behavior of the experimental and theoretical slopes is almost the same, although it should be noted that due to the uncertainty of the real area of the ink-type electrode, the number of electrons transferred per O<sub>2</sub> could not be calculated exactly. From these results, it is suggested that the O<sub>2</sub> reduction may proceed via the overall four-electron transfer reaction to water formation, i.e.  $\text{O}_2 + 4\text{H}^+ + 4\text{e}^- \rightarrow 2\text{H}_2\text{O}$ , as it was reported under the same experimental conditions from carbon paste electrodes [9,10].

The mass transfer corrected Tafel plot considering a first-order kinetic reaction, was obtained in the mixed activation-diffusion region and calculated from equation (1):

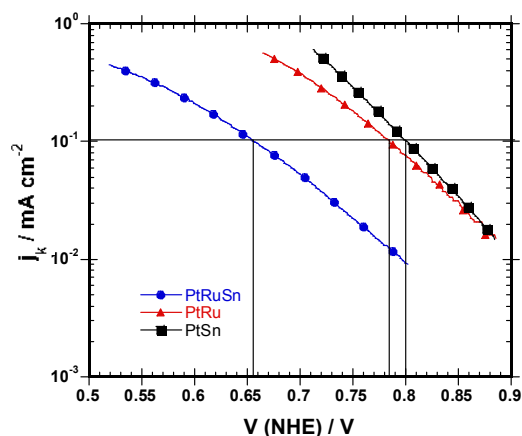


Figure 4. Mass transfer corrected Tafel plots deduced from Koutecky–Levich analysis of rotating disk current–potential data of oxygen-saturated 0.5 M H<sub>2</sub>SO<sub>4</sub> at 25°C. Vertical lines show the potential differences reached at 0.1 mA cm<sup>-2</sup>.

$$i_k = i \frac{i_d}{i_d - i} \quad (1)$$

where  $i_d/(i_d - i)$  is the mass transfer correction. The diffusion-limited density current  $i_d$  was deduced from the Koutecky–Levich plots. Figure 4 shows the mass transport corrected Tafel plots obtained for the amorphous metallic alloys PtSn, PtRu and PtRuSn ink-type catalysts deposited on glassy electrodes.

The Tafel plots show a linear behavior in the mixed activation–diffusion region and a deviation of the kinetic current occurs with higher slope at high current density. The kinetic parameters deduced for the ORR on the three amorphous electrocatalysts are presented in Table 1. It is well known that the rate of the cathodic reaction is proportional to the exchange current density and exponentially related to the Tafel slope. It is desirable to minimize the Tafel slope in order to achieve a high voltage for high operating current densities. Values of the kinetic parameters in Table 1, are consistent with that reported in literature for amorphous metallic alloys [9,10]. For practical applications, it is preferable to work at a fixed current density instead of using the value of the exchange current density due to the uncertainty of the real area of the ink-type electrode but mainly in terms of the overpotential. Figure 4 depicts also the corresponding potential attained at 0.1 mA cm<sup>-2</sup>, it is presented in Table 1. As it can be seen the PtSn amorphous electrocatalyst has the lowest overpotential at this current density and would be considered as the best from the three electrodes for the ORR in the acid electrolyte at 25°C.

### 3.3. Test performance of membrane electrode assemblies

Each MEA was prepared by spraying catalyst ink on cathodic side of the pretreated Nafion<sup>®</sup> 115 membrane. Then, the catalyzed membrane was put between porous carbon cloth for the cathode and commercial cloth electrode for the anode. The MEAs were inserted into the fuel cell for the testing processes. Studying the

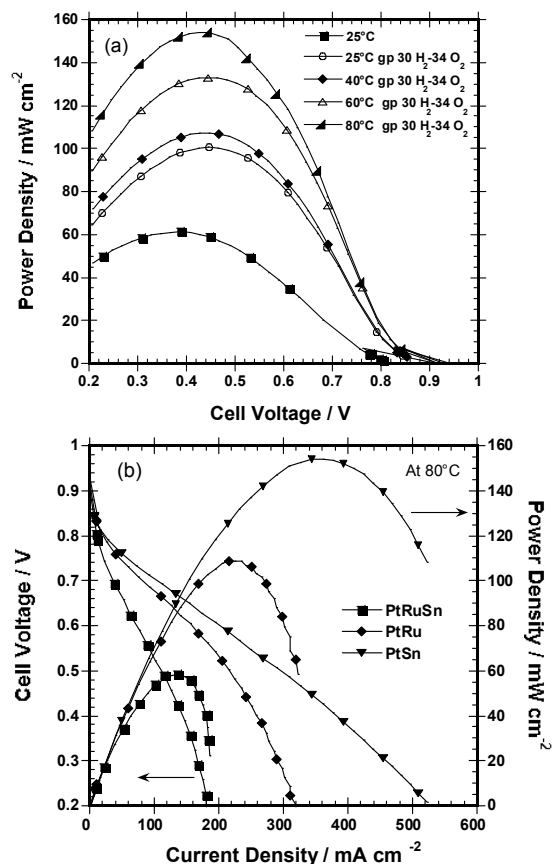


Figure 5. H<sub>2</sub>/O<sub>2</sub> PEMFC performance polarization curves: a) PtSn cathodic electrocatalyst at different temperatures and b) Curves with cathodic PtSn, PtRu and PtRuSn amorphous metallic alloys, at 80 °C.

temperature effect on the MEA performance, curves of the cell voltage and power density against current density were recorded at 25, 40, 60 and 80 °C, fed with H<sub>2</sub>/O<sub>2</sub> under 30/34 psi pressure. Figure 5(a) shows the fuel cell performance at different temperatures for the MEA, which was fabricated with a PtSn alloy cathode catalysts. An improvement of the MEA performance with an increase in the operating temperature was observed. Open circuit voltages,  $E_{oc}$  were around 0.94 V at the operating temperature. Clearly, the measured maximum power density,  $W_{max}$  was 105 mW cm<sup>-2</sup> at 40 °C, increasing to 156 mW cm<sup>-2</sup> at 80 °C, almost 50% higher than the starting current. This behavior confirms that the

oxygen reduction reaction on PtSn catalyst is activated by temperature. When compared with the single PEMFC performance for cathodes prepared with the three catalysts with platinum as anode catalyst, it is observed in figure 5(b), the kinetics of the cathode catalyst at the same temperature of 80 °C. Interesting results were obtained when comparing the performance of the PtSn catalyst with those obtained with cathodes of PtRu or PtRuSn in single fuel cells. Figure 5 (b) and data of the last two columns in Table 1 show the performances at 80 °C.

According to the performance tests, the activity of the electrocatalysts in the MEAs decreases following the next tendency: PtSn > PtRu > PtRuSn. At this point, clearly the electrocatalysts performance agrees with results of SEM and electrochemical characterization mentioned above. MEA with the best performance was reached with a cathode catalyst of PtSn reaching 156 mW cm<sup>-2</sup> at 0.43V. We know that the power density obtained with the PtSn catalyst is almost 45% lower than that obtained with commercially available platinum E-tek, under the same experimental conditions. The relatively low output performance observed with amorphous metallic PtSn, PtRu and PtRuSn alloys catalysts may be attributed basically to micro sized particles. Additional effort in catalyst preparation and assembly characterizations should be carried out to optimize the fuel cell operation.

#### 4. CONCLUSIONS

In this work amorphous metallic PtSn, PtRu and PtRuSn alloys were used as cathodes for the ORR in sulfuric acid and in a single PEM fuel cell. Two different powder morphologies were observed before and after the chemical activation in a HF 48% v/v solution. Particles before the chemical activation were spherical and compact with sizes, ranging between 5 – 30 μm. After chemical activation, the sizes were the same, but the surface was irregular and porous. Chemical activation is important because generates active sites for the cathodic reaction. Electrochemical measurements were performed with the synthesized powders and they did not present electrochemical activity. However, after chemical activation a catalytic activity is observed. PtSn amorphous electrocatalyst had the lowest overpotential at 0.1 mA cm<sup>-2</sup> on thin-film electrodes and would be considered as the best of the three electrodes for the ORR in the acid electrolyte at 25 °C. The best MEA performance was reached with a PtSn alloy cathode catalyst getting 156 mW cm<sup>-2</sup> at 0.43V. The relatively low output performance observed with amorphous metallic PtSn, PtRu and PtRuSn alloys catalysts may be attributed basically to micro sized particles. Additional effort in catalyst preparation and assembly characterizations should be carried out to optimize the cell operation.

Table 1. Kinetic parameters deduced for ORR in 0.5 M H<sub>2</sub>SO<sub>4</sub> at 25 °C and performance of amorphous metallic cathodes catalysts in a single PEMFC, at 80 °C, H<sub>2</sub>/O<sub>2</sub> under 30/34 psi pressure.

Electrocatalysts	$E_{oc}$ V/NHE	$-b$ V dec <sup>-1</sup>	$a$	$j_o$ mA cm <sup>-2</sup>	Potential (V) at $j=0.1$ mA cm <sup>-2</sup>	$P_{max}$ (mW cm <sup>-2</sup> ) at 80 °C	Voltage (V) at $P_{max}$
PtSn	0.91	0.096	0.61	$4.37 \times 10^{-6}$	0.800	156	0.43
PtRu	0.93	0.117	0.50	$1.87 \times 10^{-5}$	0.775	110	0.48
PtRuSn	0.87	0.121	0.48	$2.77 \times 10^{-6}$	0.658	60	0.45

## 5. ACKNOWLEDGEMENT

The authors gratefully acknowledge the financial support of ICYTDF (project PICS08-37), IPN (project SIP-20090433), UPV/EHU (GIU2006/2009), MEC(CTQ2006-13163/BQU). The authors wish to acknowledge to Dra. Mayahuel Ortega for technical assistance in SEM measurements.

## REFERENCES

- [1] R. Janot, D. Guérard, *Prog. Mat. Sci.*, 50, 1 (2005).
- [2] V. Collins-Martínez, R.G. González-Huerta, A. López-Ortiz, D. Delgado-Vigil, O. Solorza-Feria, *J. New Mat. Electrochem. Systems*, 12, 63 (2009).
- [3] R.G. González Huerta, A.R. Pierna, O. Solorza Feria in “Proceedings of the Simposio Ibérico de Hidrógeno, Pilas de Combustible y Baterías Avanzadas”, HYCELTEC, Bilbao, Spain, July 1-4, 2008.
- [4] P. Sotelo Mazón, R.G. González Huerta, J.G. Cabañas Moreno, O. Solorza Feria, *Int. J. Electrochem Sci.*, 2, 523 (2007).
- [5] A. Ezeta, E.M. Arce, O. Solorza, R.G. González, *J. Alloys and Compounds*, 483, 429 (2009).
- [6] L. Liu, H. Kim, J.W. Lee, B.N. Popov, *J. Electrochem. Soc.*, 154, A123 (2007).
- [7] A. Hamnett, in “Handbook of Fuel Cells, Fundamental Technology and Applications”, Ed. W Vielstich, A Lamm, H Gasteiger, John Wiley, England, 2003, Vol. 2.
- [8] Kinoshita K., in “Electrochemical Oxygen Technology”, Ed., John Wiley, 1992, ch. 1, 4.
- [9] R.G. González Huerta, A.R. Pierna, O. Solorza Feria, *J. New Mat. Electrochem. Systems*, 11, 63 (2008).
- [10] G. Ramos-Sánchez, A.R. Pierna, O. Solorza-Feria, *J. Non-Crystalline Solids*, 354, 5165 (2008).
- [11] J. Barranco, A.R. Pierna, *J. Non-Crystalline Solids*, 353, 851 (2007).
- [12] R.G. González Huerta, A. Guzmán, O. Solorza Feria, *Int. J. Hydrogen Energy*, In press 2010.